ISSN 2447-6102

Article

Numerical Simulation and Kalman-based Control of a Hall Thruster for CubeSats

Costa, H.M. [1,*], Miranda, R.A .[2], Ferreira, J.L .[3] and Muñoz, D.M. [4]

[1] University of Brasília; hudson_m.costa@outlook.com
[2] University of Brasília; rmiracer@gmail.com
[3] University of Brasília; jleonardoferreira@uol.com.br
[4] University of Brasília; damuz@unb.br
***** Correspondence: hudson_m.costa@outlook.com;

Received: Outubro/2025; Accepted: Novembro/2025; Published: Novembro/2025

Abstract: This work presents a coupled simulation framework combining a Particle-In-Cell (PIC) model and a Kalman filter-based estimator to evaluate the influence of electric propulsion on CubeSat trajectory control. A three-dimensional PIC simulation of the PHALL II-C Hall thruster was performed using a CAD model developed in SolidWorks and imported into the VSim software. From the PIC simulation, the electric and magnetic fields, electric potential, ion velocity, and thrust (64 mN) were obtained. This thrust value was then used as input for an Extended Kalman Filter (EKF) implemented in MATLAB to simulate the orbital behavior of a 6U CubeSat at 700 km altitude under continuous low-thrust conditions. The filter accurately estimated angular position, altitude, and vertical velocity over time, with low Mean Absolute Error and Root Mean Square Error values across all states. The results demonstrate the effectiveness of combining plasma simulations with state estimation techniques for nano and microsatellite mission analysis.

Keywords: Electric propulsion; satellites; Kalman Filter Extended; Particle-In-Cell simulation; Hall thrusters

1. Introduction

Hall thrusters have been used since the 1970s and remain among the most successful electric propulsion systems for space applications [1]. At the University of Brasília, the Plasma Physics Laboratory (LFP) has developed a series of Permanent Magnet Hall Thrusters (PHALL) since 2004 to support the Brazilian Space Program.

The first model, PHALL I, employed ferrite magnets and demonstrated the feasibility of using permanent magnets to generate the magnetic field. Subsequent versions evolved through different magnetic materials and configurations: PHALL II-A introduced long NdFeB magnets (1100 Gauss), PHALL II-B used shorter magnets with ferromagnetic materials (100 Gauss), and PHALL II-C incorporated SmCo magnets and a hollow cathode, achieving over 40 mN of thrust with a specific impulse of 2286 s [2-4].

To investigate this thruster's behavior, a fully 3D Particle-In-Cell (PIC) simulation was developed using a realistic CAD model of PHALL II-C. The model captures essential plasma dynamics, including ion acceleration under electric and magnetic fields, providing estimates of ion velocity and thrust [5].

The simulated thrust is then used in a Kalman Filter-based estimator to assess the orbital impact on a 6U CubeSat under continuous low-thrust conditions. This hybrid approach, combining PIC simulation and probabilistic orbit estimation, offers a practical framework for analyzing trajectory control via electric propulsion [6,7].

2. Methodology

The methodology is grounded in numerical simulation techniques. Initially, a detailed CAD model of the PHALL II-C thruster is developed using SolidWorks software. This model is then converted into STL format and imported into the

VSim software, which is employed to perform a Particle-In-Cell (PIC) simulation of the Hall thruster. From this simulation, key performance parameters, particularly the thrust, are obtained. The resulting thrust value is subsequently used as input for an Extended Kalman filter-based estimator, implemented in MATLAB, which simulates the altitude control of a CubeSat under continuous low-thrust conditions.

2.1. Particle-In-Cell (PIC) Simulation

The Fig. 1 shows the CAD model imported in the VSim software.

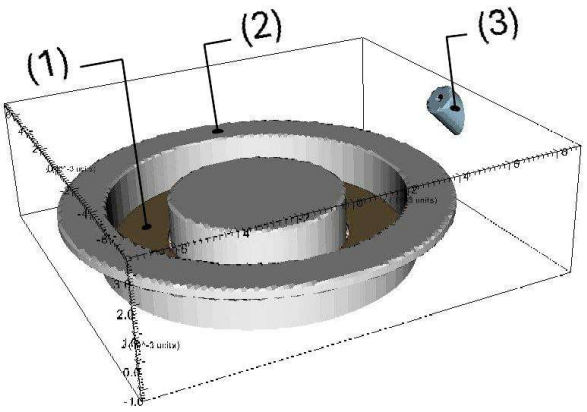

Figure 1. Isometric view of the PHALL II-C model in VSim.

In number 1 in the the Figure 1 demonstrates the dielectric body; in number 2 shows the anode; in number 3 shows the electron emitter (cathode) of the PHALL II-C. Xenon gas, which will be ionized, is injected through the lower region of the anode. Surrounding both the outer and inner surfaces of the dielectric body are permanent magnets responsible for generating the magnetic field. An electric field is established between the cathode and the anode.

According to Goebel e Katz [8], at the entrance of the dielectric channel, electrons emitted from the cathode travel toward the anode and interact with the crossed $\boldsymbol{E} \times \boldsymbol{B}$ fields, initiating a spiraling (azimuthal) motion around the dielectric channel. As the neutral xenon gas exits the dielectric body, it collides with these electrons, becoming ionized. The resulting ions are then accelerated by the electric potential established by the electric field. This electric potential is described by Eq. 1, shown below.

$$\boldsymbol{E} = -\nabla\varphi \tag{1}$$

Once the electric potential is obtained, it becomes possible to determine the velocity at which the ions exit the Hall thruster. This calculation requires the effective voltage (V_b), the charge of the ion (q), and the mass of the xenon ion (M_{Xe}). All of these parameters can be extracted from the Particle-In-Cell (PIC) simulation performed using the VSim software. Thus, the ion velocity can be calculated using Equation 2, shown below.

$$v_i = \sqrt{\frac{2qV_b}{M_{Xe}}} \tag{2}$$

Therefore, once the ion velocity is known, it is only necessary to determine the ion mass flow rate, which can also be obtained through the VSim software, to calculate the thrust produced by the PHALL II-C thruster. The thrust can then be computed using Eq. 3, as shown below.

$$\boldsymbol{T} = \dot{m}_i \boldsymbol{v}_i \tag{3}$$

2.2. Extended Kalman Filter (EKF) simulation

The Extended Kalman filter is applied to a scenario involving a nano or microsatellite, specifically, a 6U CubeSat, in orbit around the Earth. In this study, the satellite is assumed to be in a circular orbit at an altitude (R) of 700 km, with a

total mass (m) of 10 kg. To determine the satellite's tangential velocity, we use Eq. 4, where G is the universal gravitational constant, M_T is the mass of the Earth, and r is the orbital radius (radius of the Earth + R). The thrust value (T) used in the model is obtained from the PIC simulation of the PHALL II-C thruster.

$$v_T = \sqrt{\frac{GM_T}{r}} \tag{4}$$

Consequently, the initial conditions and input parameters employed in the Extended Kalman filter (EKF) algorithm are summarized in Table 1.

Table 1. Initial conditions for the Extended Kalman filter (EKF) algorithm.

Variables	Value
R	700 km
T	PIC simulation
m	10 kg
v_T	7.51 km/s

Consider a two-dimensional representation of the Earth as a circle. Orbiting around it, at an altitude of 700 km from the Earth's surface, is a CubeSat. The position of this CubeSat in the orbital plane is described by Equations 5 and 6.

$$x = R\cos\theta \tag{5}$$

$$y = R\sin\theta \tag{6}$$

To avoid quadrant ambiguity, the angular position is defined with the two-argument arctangent:

$$\dot{\theta} = \mathrm{atan2}(y, x) \tag{7}$$

Differentiating, the angular rate is:

$$\dot{\theta} = \frac{x\dot{y} - y\dot{x}}{x^2 + y^2} \tag{8}$$

which, for an (approximately) circular orbit where $x^2 + y^2 \approx R^2$, is consistent with $\dot{\theta} \approx v_T/R$.

Consequently, the velocity components in the x and y directions are given by Equations 9 and 10, respectively:

$$\dot{x} = -\dot{\theta}R\sin\theta \tag{9}$$

$$\dot{y} = \dot{\theta}R\cos\theta \tag{10}$$

Based on these relations, the initial state vector ($\boldsymbol{x}$), the state transition function ($\boldsymbol{f}$), and the measurement function ($\boldsymbol{g}$) are defined as follows:

$$\boldsymbol{x} = \begin{bmatrix} R\cos\theta \\ R\sin\theta \\ z \\ -\theta R\dot{\sin}\theta \\ \dot{\theta}R\cos\theta \\ \dot{z} \end{bmatrix} \qquad \boldsymbol{f} = \begin{bmatrix} R\cos(\theta + \dot{\theta}dt) \\ R\sin(\theta + \dot{\theta}dt) \\ z + \dot{z}dt + 0.5(T/m)dt^2 \\ -\theta R\,\mathrm{sin}(\dot{\theta} + \dot{\theta}dt) \\ \dot{\theta}R\cos(\theta + \dot{\theta}dt) \\ \dot{z} + (T/m)dt \end{bmatrix} \qquad \boldsymbol{g} = \begin{bmatrix} R\cos\theta \\ R\sin\theta \\ z \\ -\theta R\dot{\sin}\theta \\ \dot{\theta}R\cos\theta \\ \dot{z} \end{bmatrix}$$

Where z is the altitude correction value.

3. Results and Discussion

In this section, we present and discuss the results obtained from the Particle-In-Cell (PIC) simulation and the Kalman filter algorithm.

3.1. Particle-In-Cell (PIC) simulation results

The PIC simulation provides the magnetic and electric fields, the electric potential, and the resulting thrust produced by the thruster.

3.1.1. Magnetic and Electric field

The Figures 2 and 3 show the topology of the magnetic field lines and the electric field lines.

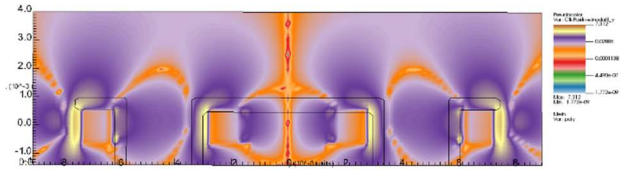

Figure 2. Topology of magnetic field lines.

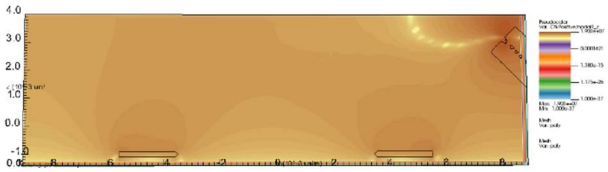

Figure 3. Topology of electric field lines.

By drawing a vertical line at the propellant gas outlet, it is possible to analyze the profiles of the radial magnetic field and the axial electric field as functions of the axial position. These results are presented in Figures 4 and 5.

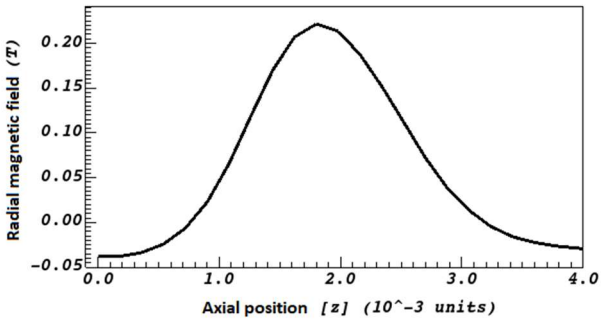

Figure 4. Radial magnetic field versus axial position.

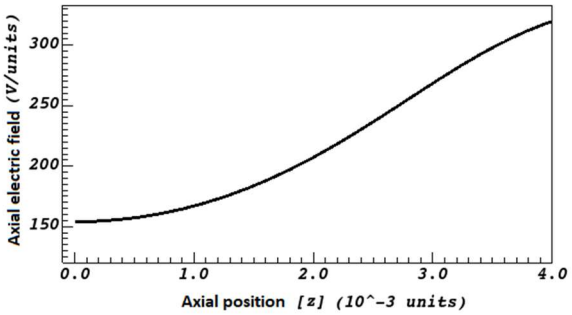

Figure 5. Axial electric field versus axial position.

By analyzing the figures that show the behavior of the electric and magnetic fields, we observe that the results are consistent with theoretical predictions. The fields exhibit a distribution such that the crossed $\boldsymbol{E} \times \boldsymbol{B}$ fields at the thruster outlet induce a circular motion of the electrons near the thruster entrance, thereby generating the Hall current and facilitating ionization.

3.1.2. Electric potential

The Figure 6 show the topology of the electric potential field.

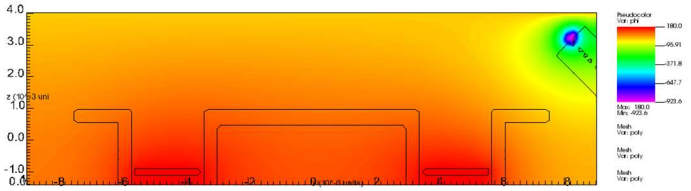

Figure 6. Topology of electric potential.

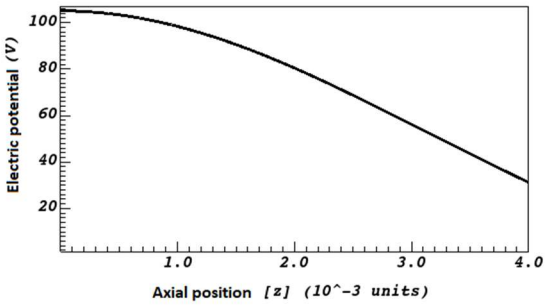

Figure 7. Electric potential versus axial position.

By drawing a vertical line at the propellant gas outlet, we obtain the profile of the electric potential as a function of the axial position. This profile is crucial for calculating the ion velocity, as it allows us to determine the effective voltage. Specifically, we take the maximum value of the electric potential from this profile, which is 106 V, and divide it by the square root of 2 to find the effective voltage.

3.1.3. Thrust calculation

Figure 8 shows the histogram of ion particles as a function of time, that is, the number of particles per second, which is 2.8×10^{19} particles/s. To calculate the mass flow rate in kilograms per second (kg/s), we simply multiply this value by the mass of a single xenon atom (M_{Xe}), yielding the mass flow rate.

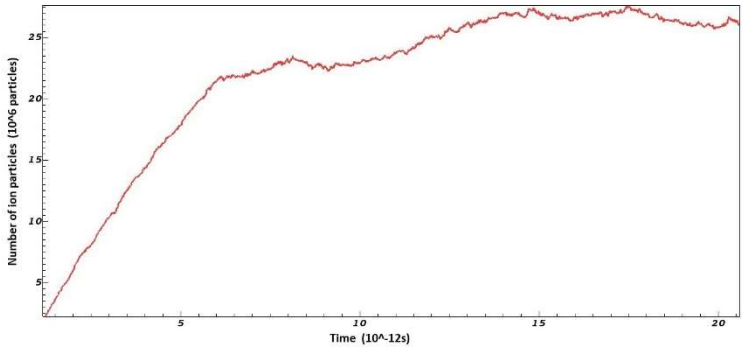

Figure 8. Histogram of ion particles versus time.

In this way, Table 2 presents the equation used to calculate the ion velocity.

Table 2. Ion velocity equation parameters.

Variables	Value
q	$+1.6 \times 10^{-19}\ C$
V_b	$75\ V$
M_{Xe}	$2.180 \times 10^{-25}\ kg/particle$

Using Eq. 2, the ion velocity (v_i) is calculated to be 10,492.46 m/s. Based on Fig. 8 and the xenon atomic mass (M_{Xe}) provided in Table 2, the mass flow rate ($\dot{m}_i$) is determined to be 6.10×10^{-6} kg/s. Therefore, applying Eq. 3, the resulting thrust (T) is 64 mN.

3.2. Extended Kalman filter (EKF) estimation results

Using the data from Table 1 and the thrust value obtained from the PIC simulation, we estimated and compared the angular variation, vertical velocity, and altitude after 15 minutes of thruster operation with their corresponding true values. Here, the term true value refers to the reference trajectory generated directly from the nonlinear system

dynamics with process noise, which serves as the ground truth against which the Extended Kalman Filter (EKF) estimates are validated. These results are shown in Figure 9.

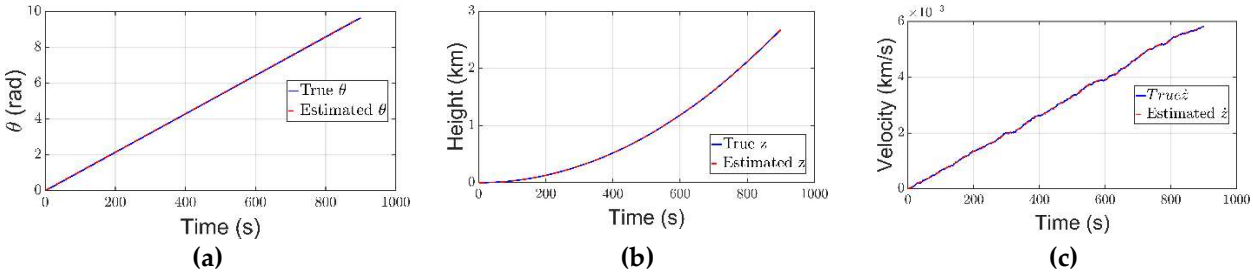

Figure 9. Extended Kalman filter (EKF) estimation results: **(a)** Comparison between true and estimated θ; **(b)** Comparison between true and estimated height z; **(c)** Comparison between true and estimated velocity z.

Figure 9a presents the comparison between the true and estimated angular variation of the CubeSat's position. Figure 9b shows the comparison between the true and estimated altitude variation, relative to the initial altitude of 700 km. Finally, Figure 9c displays the vertical velocity profile over time.

After 15 minutes of thruster operation, the CubeSat experienced an angular variation of approximately 9.8 radians. The vertical velocity also increased due to the continuous thrust, resulting in an estimated altitude gain of about 2.6 km by the end of the simulation.

Table 3. Statistical error metrics for Extended Kalman filter (EKF) estimation.

Variables	MAE	RMSE
$\theta\ (rad)$	1.2971×10^{-2}	1.3056×10^{-2}
$Z\ (km)$	1.0808×10^{-4}	1.3151×10^{-4}
$V_z\ (km/s)$	1.1685×10^{-5}	1.4394×10^{-5}

The performance of the Extended Kalman Filter (EKF) was evaluated using the Mean Absolute Error (MAE) and Root Mean Square Error (RMSE). The results indicate consistently low errors: for the angular position, MAE = 1.2971×10^{-2}rad and RMSE = 1.3056×10^{-2} rad (≈ 0.74-0.75°); for altitude, MAE =1.0808×10^{-4} km and RMSE = 1.3151×10^{-4} km (≈ 0.11-0.13 m), and for vertical velocity, MAE = 1.1685×10^{-5}km/s and RMSE = 1.4394×10^{-5} km/s (≈ 0.012-0.014 m/s). These figures confirm that the EKF maintained high estimation accuracy throughout the simulation.

4. Discussion

The PIC simulation results align with Hall thruster physics, confirming effective ion acceleration under crossed $\boldsymbol{E} \times \boldsymbol{B}$ fields near the channel exit. The electric field profile indicates that most acceleration occurs in the final region of the discharge channel, as expected.

The thrust magnitude obtained (64 mN) is consistent with values reported experimentally for PHALL II-C, validating the simulation approach.

When this thrust is injected into the EKF orbital model, it demonstrates meaningful trajectory correction capability for CubeSat-class satellites. The predicted altitude gain (2.6 km in 15 min) confirms the feasibility of low-thrust orbital adjustments in short time intervals.

Moreover, the EKF maintained strong estimation convergence, with angular, altitude, and velocity errors staying close to zero throughout the simulation, showing that state estimation remains reliable despite nonlinear orbital dynamics.

5. Conclusions

This study successfully integrated a high-fidelity PIC simulation with an Extended Kalman Filter to analyze the impact of continuous low-thrust propulsion on CubeSat orbital control. The 3D PIC model accurately reproduced the internal behavior of the PHALL II-C Hall thruster, providing consistent physical results in line with theoretical expectations, particularly regarding $\boldsymbol{E} \times \boldsymbol{B}$ field behavior and ion acceleration. The calculated ion velocity and mass

flow rate resulted in a thrust of 64 mN, which was used to simulate the orbital response of a 6U CubeSat. The Kalman filter showed strong estimation performance, with an angular variation of 9.8 radians and an altitude increase of 2.6 km over 15 minutes, all with minimal statistical error. These results confirm the feasibility of combining PIC-based propulsion modeling with probabilistic state estimation to support the development and control of electric propulsion systems for nano and microsatellites.

Funding: This work was supported by the National Council for Scientific and Technological Development (CNPq) through the project "Development of Hall-effect Electric Propulsion Systems for Nano and Micro-satellites" under the CNPq Call No. 20/2022 – Category B. The project received financial support and student scholarships from CNPq, Federal District Research Support Foundation (FAP-DF), and the Brazilian Space Agency (AEB) through their institutional funding programs.

Acknowledgments: The author gratefully acknowledges Dr. Carlos Humberto Llanos Quintero for his valuable guidance during the initial development of both simulations. His contributions were fundamental to the early stages of this work, and his memory is honored through its continuation. RAM acknowledges support from CNPq, Brazil (grants 407341/2022-6, 407493/2022-0), FAPDF, Brazil (grant 383/2023) and the Brazilian Space Agency (TED 000529/2024). JLF acknowledges support from CNPq (grant 05907/2022-2) and the Brazilian Space Agency (TED 000529/2024).

Conflicts of Interest: The authors declare no conflict of interest.

References

1. KOKAL, U. et al. Development of the new bustlab hall thruster with internal coaxial hollow cathode. In: *53rd AIAA/SAE/ASEE Joint Propulsion Conference.* [S.l.: s.n.], **2017**. p. 4810.
2. MARTINS, A. et al. Preliminary experimental results of the phall ii-c with improved magnetic circuit design and hollow cathode. In: IOP PUBLISHING. *Journal of Physics: Conference Series.* [S.l.], **2019**. v. 1365, n. 1, p. 012025.
3. MARTINS, A. A.; RODRIGO, M.; FERREIRA, J. L. Magnetic field design for a strongly improved phall thruster. In: IOP PUBLISHING. *Journal of Physics: Conference Series.* [S.l.], **2017**. v. 911, n. 1, p. 012024.
4. FERREIRA, J. L. et al. Development of a solar electric propulsion system for the first brazilian deep space mission iepc-2017-166. **2017**.
5. LAPENTA, G. Particle in cell methods with application to simulations in space weather. *Centrum voor Plasma Astrofysica.–Leuven*, **2010**.
6. KALMAN, R. E. A new approach to linear filtering and prediction problems. **1960**.
7. BROWN, R. G.; HWANG, P. Y. Introduction to random signals and applied kalman filtering: with matlab exercises and solutions. *Introduction to random signals and applied Kalman filtering: with MATLAB exercises and solutions*, **1997**.
8. GOEBEL, D. M.; KATZ, I. *Fundamentals of electric propulsion: ion and Hall thrusters*. [S.l.]: John Wiley & Sons, **2008**.